

Supporting Information

Large-scale facile-synthesis and bistable emissions of one-dimensional organic-inorganic $C_4H_{14}N_2PbBr_4$ metal halide crystals with bipolaronic states

Hui Peng,^{a,b} Ye Tian,^a Xinxin Wang,^a Shangfei Yao,^b Tao Huang,^b Yongchang Guo,^a Lijie Shi^a
and Bingsuo Zou^{b*}

¹Beijing Key Laboratory of Nanophotonics & Ultrafine Optoelectronic Systems, Beijing Institute of Technology, Beijing 100081, China.

²Guangxi Key Lab of Processing for Nonferrous Metals and Featured Materials and Key Lab of New Processing Technology for Nonferrous Metals and Materials, Ministry of Education, School of Resources, Environments and Materials, Guangxi University, Nanning 530004, China.

***Corresponding Author.**

E-mail addresses: zoubs@gxu.edu.cn (B. S. Zou).

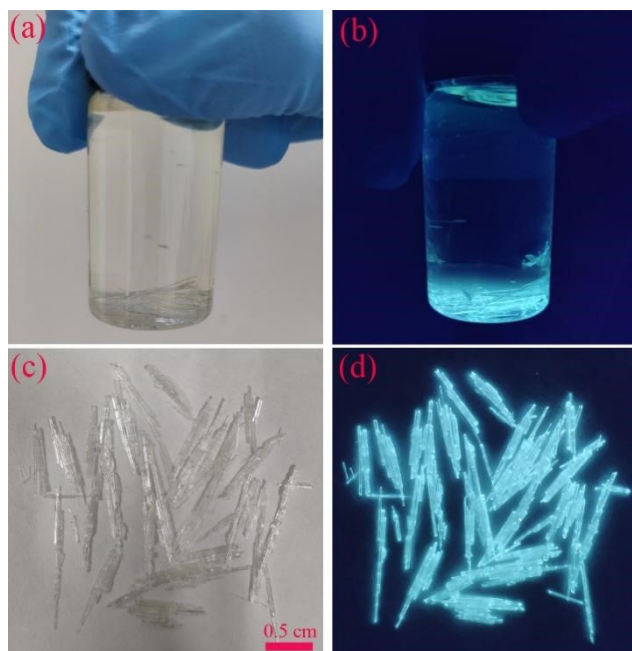


Fig. S1 Images of bulk crystals of Sample 1 under ambient light (a, c) and 365 nm UV light (b, d).

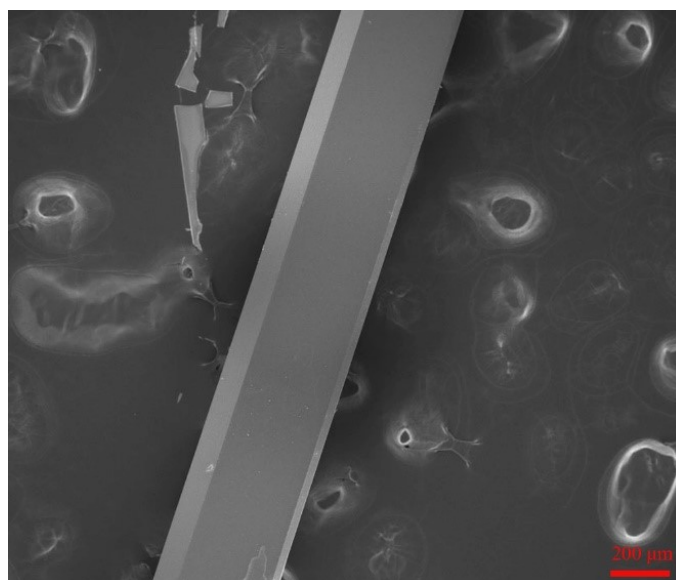


Fig. S2 SEM image of Sample 1.

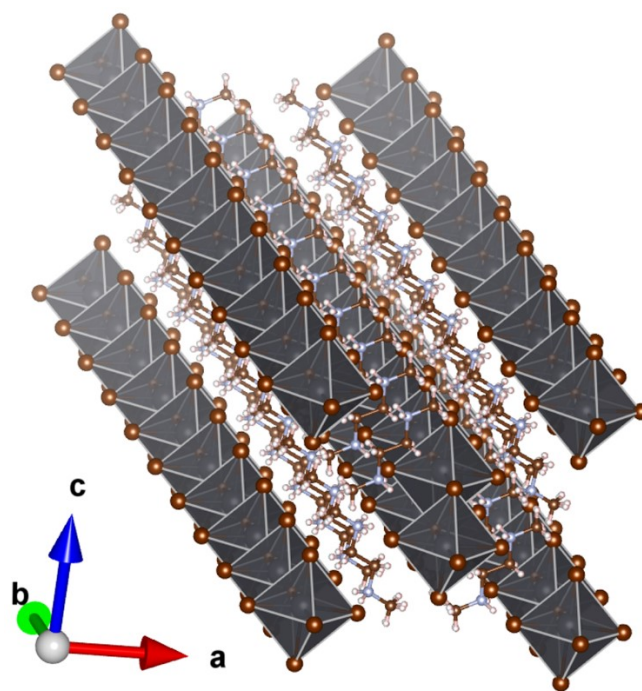


Fig. S3 View of lead bromide quantum wire wrapped by $C_4H_{14}N_2^{2+}$ organic cations.

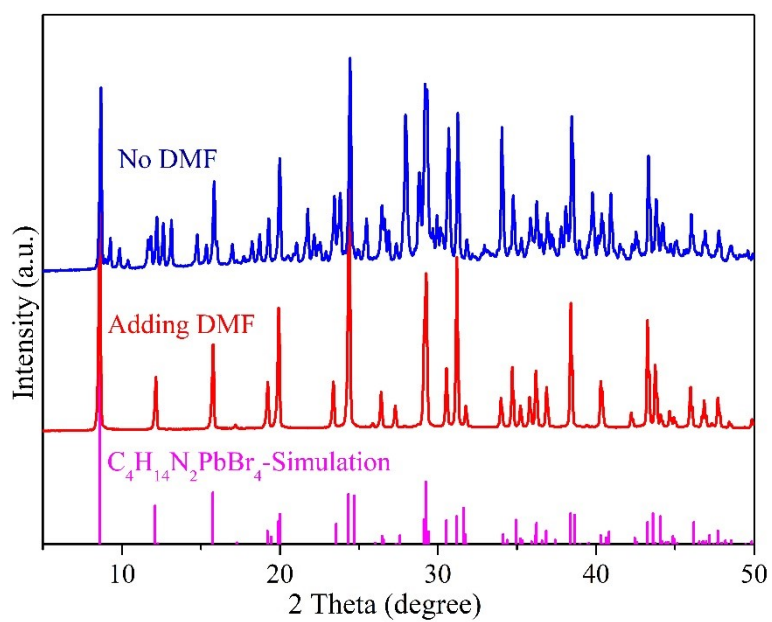


Fig. S4 PXRD patterns of the Sample 3 before and after adding DMF.

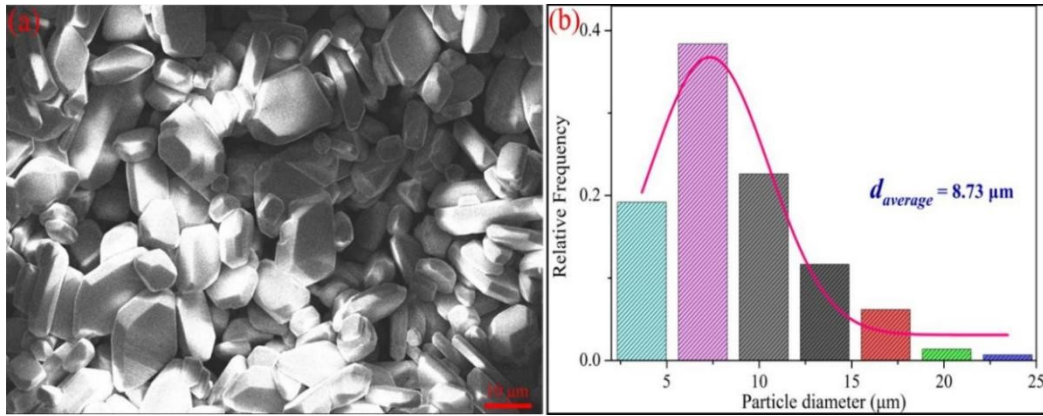


Fig. S5 (a) SEM image of Sample 2 and (b) corresponding particle size distribution

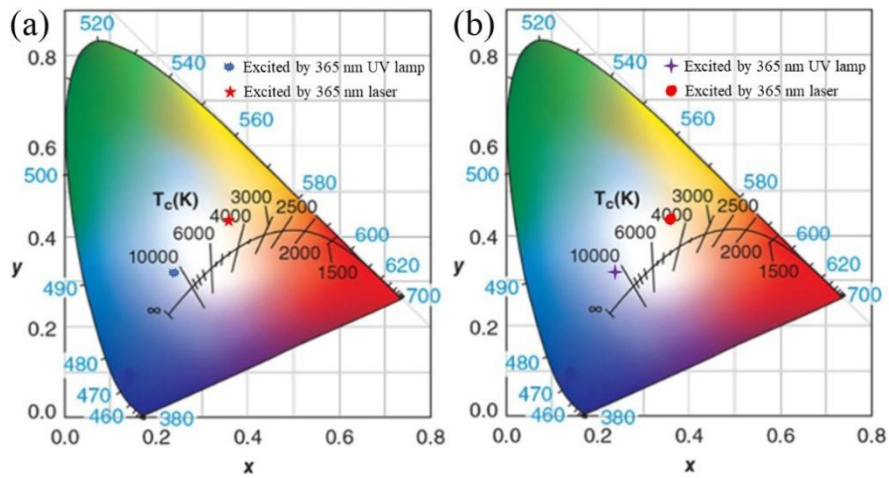


Fig. S6 The CIE chromaticity diagram of Sample 1 (a) and Sample 2 (b) excited by 365 nm UV lamp and 365 nm laser, respectively. The chromaticity coordinate of the Sample 1 is (0.241, 0.318) and (0.362, 0.437), while that of sample 2 is (0.241, 0.317) and (0.362, 0.438).

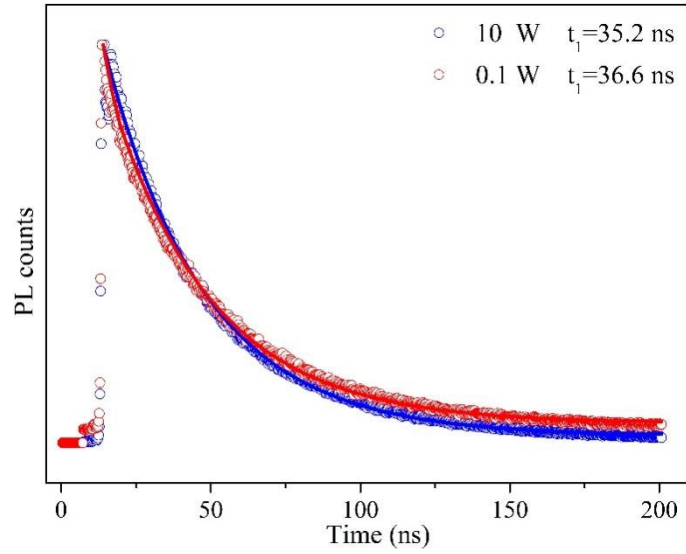


Fig. S7 The PL decay lifetime curves (monitored at 546 nm) of Sample 3 at different excitation powers (excited by 365 nm laser).

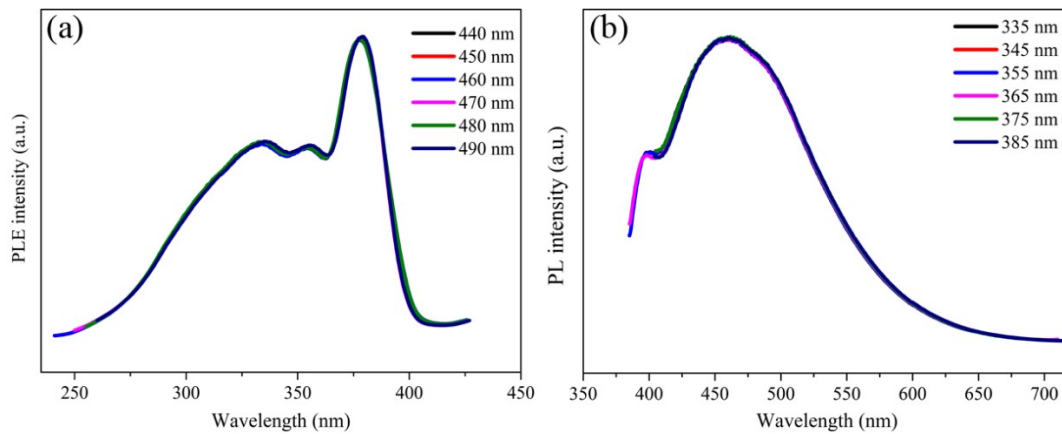


Fig. S8 Emission-wavelength-dependent photoluminescence excitation (PLE) and excitation-wavelength dependent PL spectra of Sample 3.

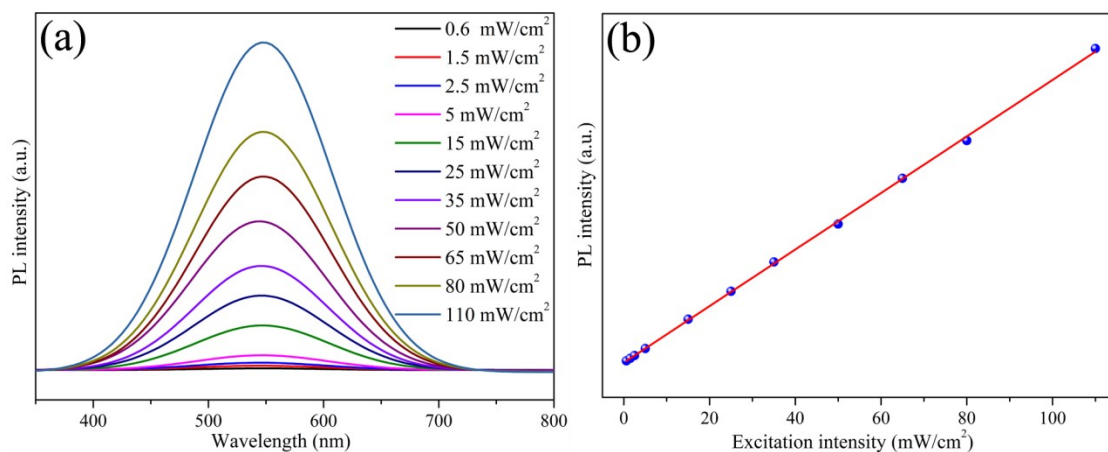


Fig. S9 (a) Power dependence PL spectra for Sample 3. (b) The PL intensity versus excitation power of Sample 3.

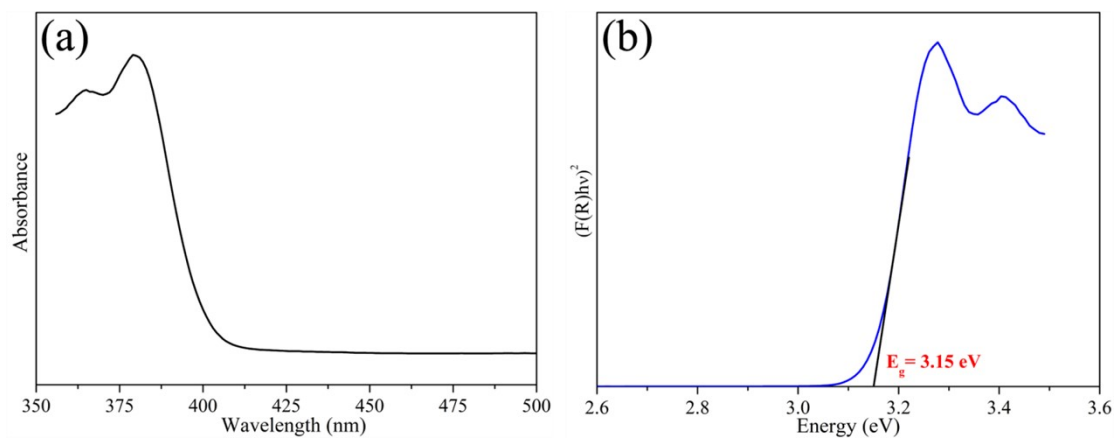


Fig. S10 UV-visible absorption spectrum of Sample 3 at room temperature. (b) The band gap of Sample 3 determined from a Tauc plot with a band gap of 3.15 eV.

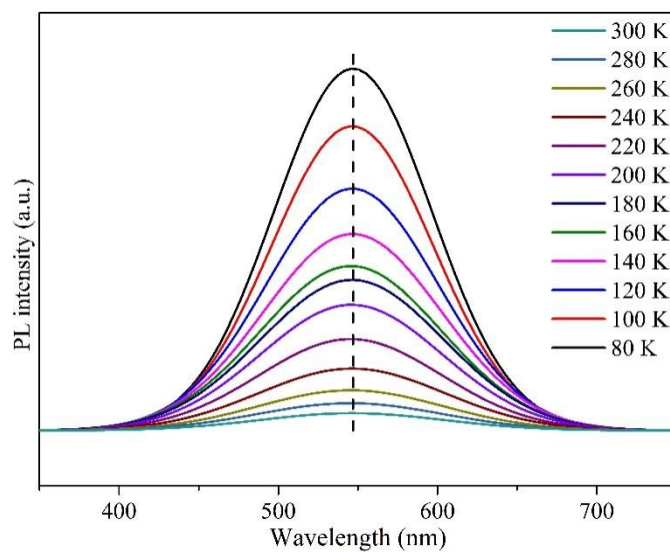


Fig. S11. Temperature-dependent PL of Sample 1 in the temperature range of 80-300 K.

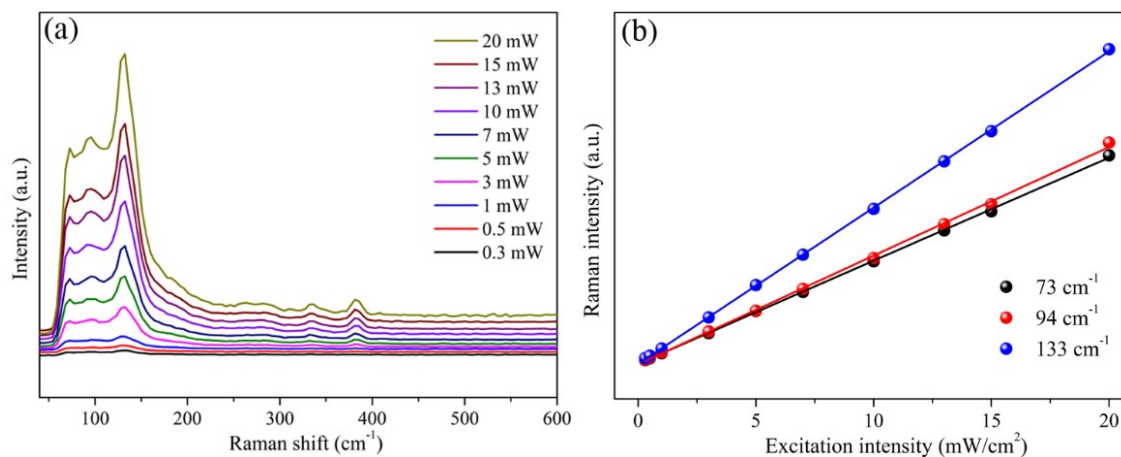


Fig. S12 (a) The Raman spectra of Sample 3 at different excitation powers. (b) The Raman intensity versus excitation power of Sample 3.

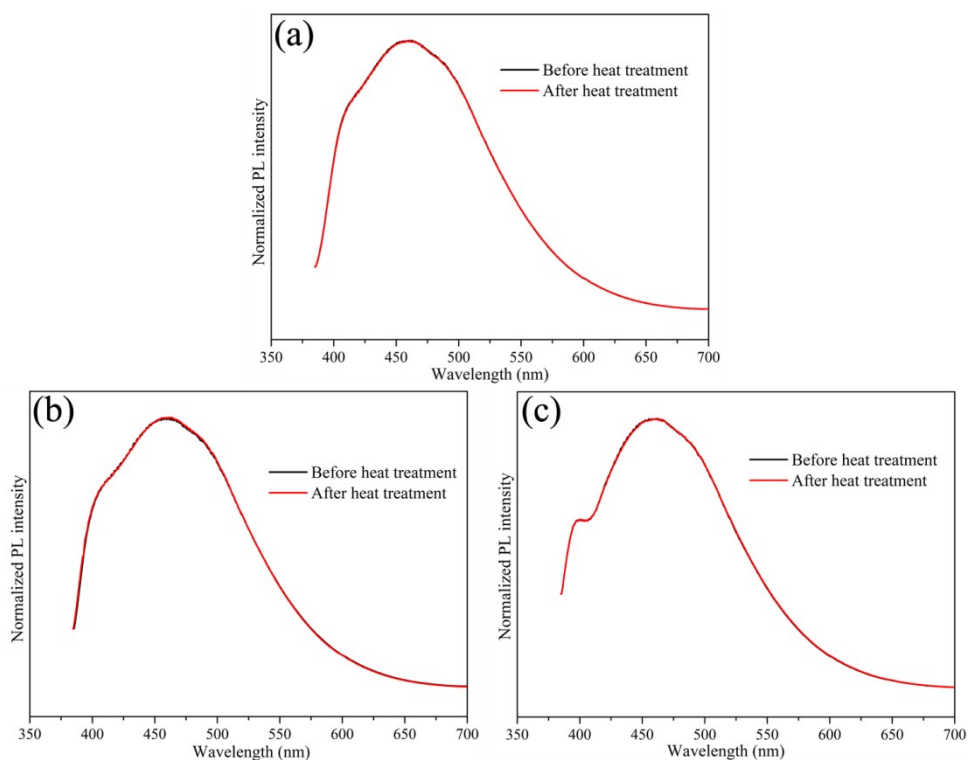


Fig. S13 The PL spectra of Sample 1 (a), Sample 2 (b), and Sample 3 (c) before and after before and after heat treatment at 100 °C for 30 minutes.

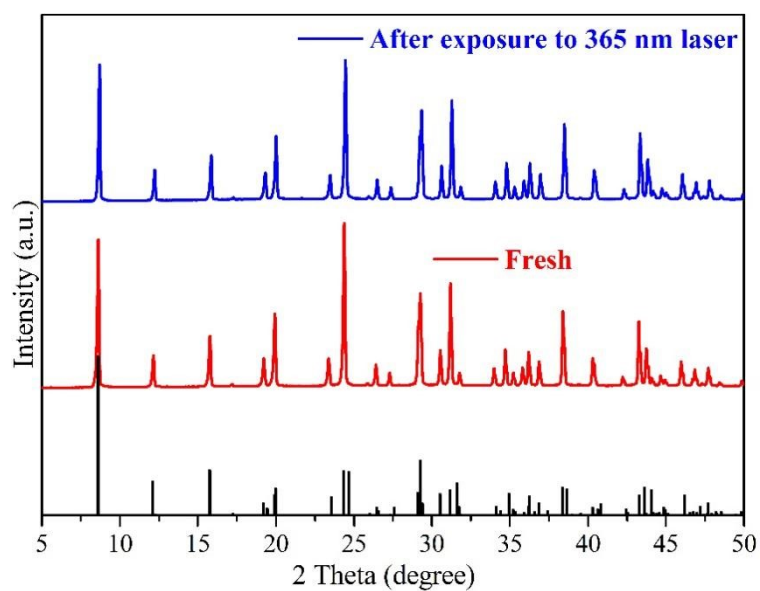


Fig. S14 PXRD patterns of Sample 3 before and after exposure to 365 nm laser.

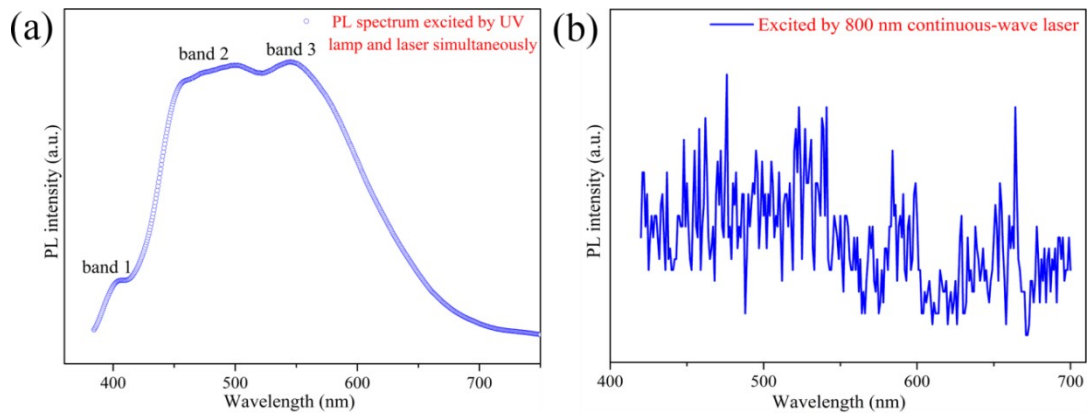


Fig. S15 (a) PL spectrum of $C_4H_{14}N_2PbBr_4$ excited by UV lamp and laser simultaneously. (b) PL spectrum of $C_4H_{14}N_2PbBr_4$ excited by 800 nm continuous-wave laser.

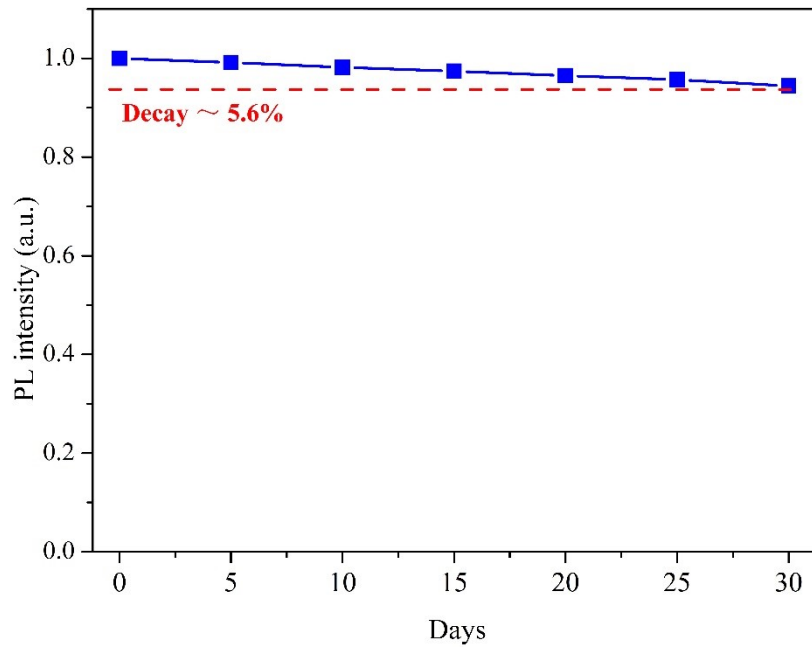


Fig. S16 The PL intensity of Sample 3 at different times within one month.

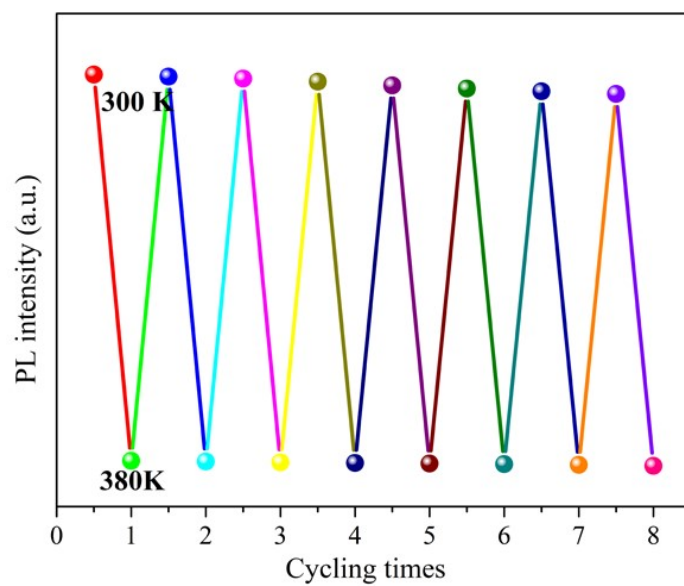


Fig. S17 Temperature-dependent PL intensity of Sample 3 alternating between 80 K and 300 K.

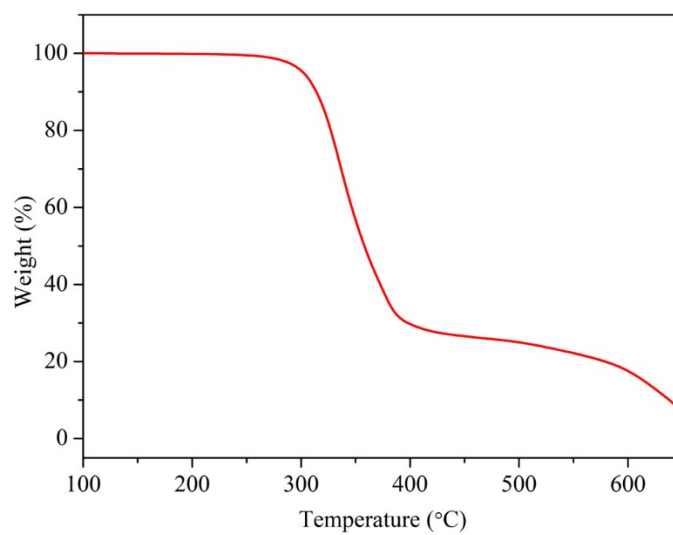


Fig. S18 TG curve of $C_4H_{14}N_2PbBr_4$ powders

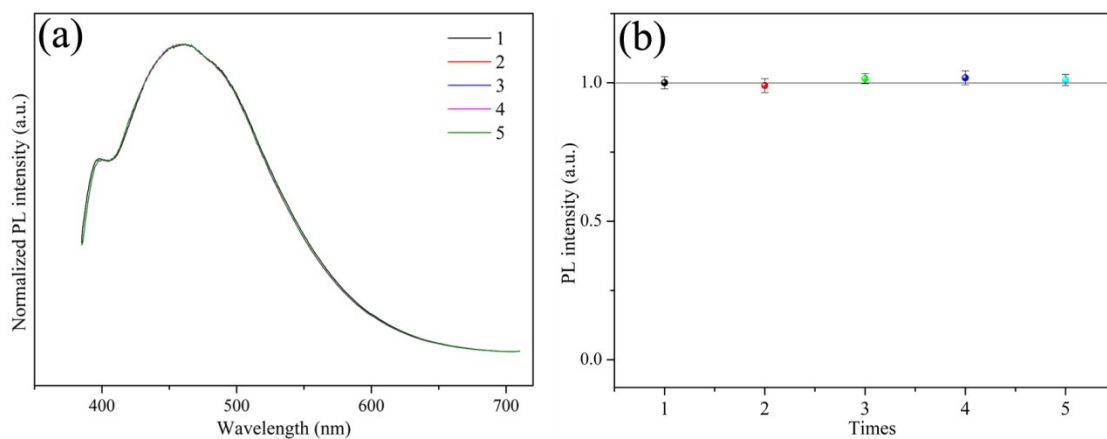


Fig. S19 (a) The emission spectra and corresponding PL intensity (b) of five different batches of Samples 3 under the same conditions.

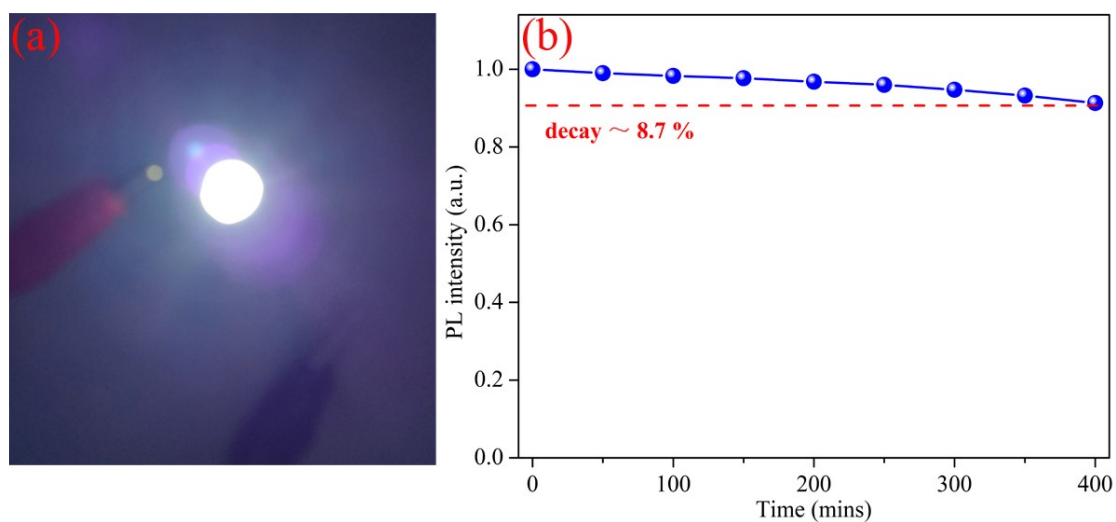


Fig. S20 (a) A bright bluish white-light emission of Sample 3 was excited by 365 nm commercially available UV chip. (b) The PL intensity of Sample 3 under continuous illumination using a 365 nm UV chip within 400 minutes.